Estimating Reflectivity by Non-stationary Deconvolution of Ultra-wide Band Radar Data: Application to Microwave Breast Imaging

Kay Yuhong Liu[*1], *Elise C. Fear*[1], *and Mike Potter*[1]

[1]Schulich School of Engineering, University of Calgary, 2500 University Drive NW, Calgary, Alberta Canada T2N 1N4
phone: 01-403-210-5418, fax: 01-403-282-6855, email: yuliu@ucalgary.ca, fear@ucalgary.ca, mpotter@ucalgary.ca

Abstract

The quality of a microwave breast image is gaged in part by the resolution of the recorded scatter fields. Deconvolution is applied to improve the signal resolution and yield a representation of subsurface reflectivity by compressing the excitation pulse in the recorded signals. As the electromagnetic wave propagates through lossy and dispersive breast tissues, the waveform is distorted due to the frequency dependent attenuation. This imposes challenges on the stationary deconvolution techniques, which assume a time-invariant propagating wavelet. In this paper, we apply Gabor non-stationary deconvolution to compensate for these dissipative and dispersive effects. Results demonstrate that this method provides a more accurate estimate of the reflectivity of the imaged object and shows ability to compensate for the wave attenuation and correct the waveform distortion.

1. Introduction

Consideration of the sensitivity, specificity, cost, and availability of established breast screening methods motivates interest in alternative or complementary technologies. The last decade has seen growing investigation of imaging techniques with low-power, microwave-frequency electromagnetic (EM) waves. In microwave imaging, a breast under investigation is illuminated with EM fields at microwave frequencies. The distribution of the fields depend on the dielectric properties of the breast tissues [1]. Malignant tissues have different permittivities and conductivities from healthy breast tissues; therefore these tissues will scatter differently, indicating their presence. The quality of a microwave image is gaged by the resolution of recorded signal. A broadband spectrum is required in order to achieve a high resolution. Among the methods that are employed to broaden the frequency bandwidth, deconvolution has demonstrated efficiency.

The recorded signal is modeled as the convolution between the excitation pulse and the reflectivity function of the imaged object [2, 3]. Deconvolution, as an inverse operation of convolution, improves the signal resolution and yields a representation of subsurface reflectivity by compressing the excitation pulse and attenuating reverberations in the recorded signal [2]. A stationary convolutional model assumes that the source wavelet does not evolve with distance traveled and the pulse is reflected or transmitted without distortion. However, this assumption is only a simplification of the actual wave propagation. Over microwave frequencies, most body tissues are lossy and dispersive. The attenuation constant and the phase velocity are frequency-dependent. This dependence is such that the high-frequency components of the spectra travel with a higher velocity and are more quickly attenuated than the low frequency ones. The dissipative and dispersive effects caused by this frequency dependence introduce continuous changes in both amplitude and phase spectra of the EM pulse. As a result, the excitation pulse often undergoes a significant distortion in shape as it travels through the media, and the received signals at later times are noticeably broader than those received at earlier times. The non-stationary behavior imposes challenges to stationary deconvolution. Therefore, a non-stationary convolutional model is necessary in order to account for those significant changes in the waveform.

In this paper, we propose the Gabor non-stationary deconvolution technique [4] to handle the waveform distortion in those challenging scenarios. Motivated by the constant Q theory [5], the Gabor algorithm was developed to deal with the non-stationarity in the recorded seismogram for geophysical imaging. With a constant Q model, the wave propagation and attenuation are characterized by a dimensionless and frequency-independent parameter, Q. The Gabor algorithm transforms the signal into Gabor domain (time-frequency domain), estimates the impulse response of wave attenuation and dispersion at given travel locations, and convolves the impulse response with the excitation pulse to capture the distorted waveform. Compared to the stationary deconvolution, a significant improvement in the estimated reflectivity function has been observed with Gabor deconvolution in the presence of waveform distortion.

The rest of the paper is organized as follows. In section 2, we briefly review the principle and the workflow of Gabor deconvolution. In section 3, the analytic model to generate the synthetic data is described, and the Gabor algorithm is shown to yield more accurate estimates of the reflectivity function than one of the widely used deconvolution methods, i.e., Wiener deconvolution. Finally, in Conclusions, results are summarized and future work is discussed.

2. Gabor Non-stationary Deconvolution

2.1 The Principles

978-1-4673-5225-3/14/$31.00 ©2014 IEEE

In its simplest form, the stationary convolutional model of a recorded signal *s(t)* is often stated as

$$s(t) = w(t) * r(t)\,, \tag{1}$$

where *w(t)* is the excitation pulse and *r(t)* is the reflectivity function. To model the wavelet distortion, Gabor deconvolution is using a non-stationary convolutional model, in which the attenuation is included as a separated effect from the excitation pulse

$$s(t) = w(t) * b(\tau, t) * r(t)\,, \tag{2}$$

where $b(\tau, t)$ is the impulse response of the attenuation process for any travel time τ. In frequency domain, equation (2) is expressed as

$$S(\omega) = W(\omega)B(\tau, \omega)R(\omega)\,, \tag{3}$$

where $S(\omega)$, $W(\omega)$, $B(\tau, \omega)$, and $R(\omega)$ are the Fourier transforms of $s(t)$, $w(t)$, $b(\tau, t)$, and $r(t)$, respectively. The goal of Gabor deconvolution is to estimate the reflectivity function

$$R(\omega) = \frac{S(\omega)}{W(\omega)B(\tau, \omega)}\,. \tag{4}$$

Gabor non-stationary deconvolution relies on the following assumptions: 1) the excitation pulse is minimum phase [6]; 2) the wave attenuation can be characterized by a frequency-dependent, minimum-phase amplitude loss [7, 8]; 3) the wave attenuation can be described by constant Q theory [5]; and 4) the amplitude spectrum of the reflectivity function is approximately constant, i.e., white reflectivity. Using the two minimum phase assumptions, we only need to estimate the amplitude spectrum of each component on the right hand side of equation (4) since the phase spectrum is computable as the Hilbert transform (over frequency) of the natural logarithm of the amplitude [9]. With the assumption of constant Q attenuation, the amplitude of $B(\tau, \omega)$ is given by

$$\left|B(\tau,\omega)\right| = e^{-|\omega|\tau/(2Q)}\,, \tag{5}$$

in which the dimensionless measure Q is the ratio between the stored energy and the lost energy in one wave cycle [10]. Q is usually given by

$$Q = \omega/(2v\alpha)\,, \tag{6}$$

where v is the phase velocity and α is the attenuation coefficient. The assumption of white reflectivity is necessary for the case that the excitation pulse $W(\omega)$ is unknown and needs to be estimated. This assumption enables us to estimate the amplitude spectrum of the unknown excitation pulse by smoothing the amplitude spectrum of the recorded data after the attenuation loss has been compensated:

$$\left|W(\omega)\right| = \left[\left|S(\omega)\right|/\left|B(\tau,\omega)\right|\right]/a\,, \tag{7}$$

where a is a constant value to represent the amplitude spectrum of $R(\omega)$.

2.2 The Workflow

The Gabor algorithm estimates the amplitude of the attenuation function $B(\tau, \omega)$ in Gabor domain based on the time-frequency decomposition of recorded data. First, a set of windows in the signal are constructed using the partition of unity (POU) scheme [4]. A POU is a set of localizing windows within which the propagating wavelet is assumed to be stationary and their superposition sums to unity. Inside each POU window, the signal is transformed to Gabor domain:

$$\hat{S}_g(t_k, \omega) \approx \hat{W}(\omega)B(t_k, \omega)\hat{R}_g(t_k, \omega)\,, \tag{8}$$

where t_k is the centre of a POU window, $\hat{S}_g(t_k, \omega)$ is the Gabor transform of the windowed signal, $\hat{W}(\omega)$ is the Fourier transform of the source wavelet and is time-independent, $B(t_k, \omega)$ is the attenuation function at time t_k, and $\hat{R}_g(t_k, \omega)$ is the Gabor transform of the windowed reflectivity. Figure 1 shows the magnitude of the four components in equation (8) for the particular case of a non-stationary synthetic signal. Equation (5) implies that hyperbolic contours, i.e., $\tau\omega$=constant, representing the level of amplitude loss can be constructed in the t-ω plane in the Gabor domain. Thus, $|B(t_k, \omega)|$ is estimated by hyperbolic smoothing [4], meaning averaging along those hyperbolic contours of $|\hat{S}_g(t_k, \omega)|$. Given $|B(t_k, \omega)|$, $|\hat{W}(\omega)|$ is then estimated by averaging $|\hat{S}_g(t_k, \omega)|/|B(t_k, \omega)|$ over time and then smoothing the result in frequency. Since $\hat{W}(\omega)$ and $B(t_k, \omega)$ are minimum phase, the phase of $\hat{W}(\omega)B(t_k, \omega)$ is determined as

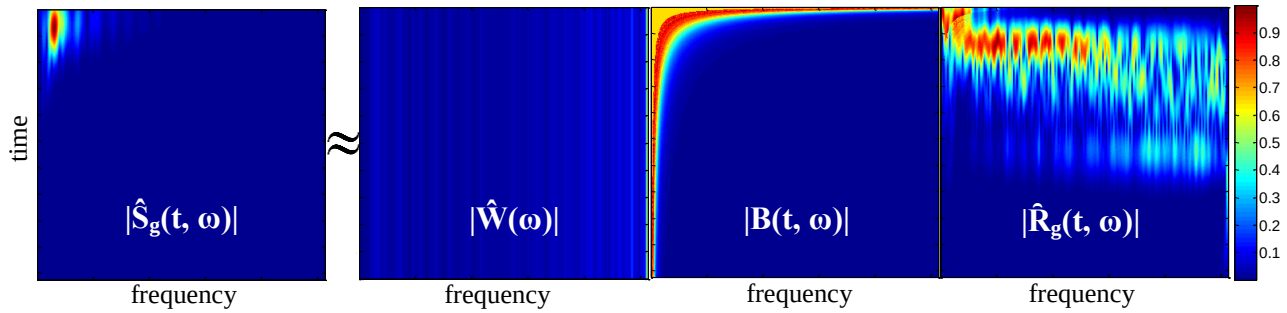

Figure 1 The normalized magnitude of the four components in equation (8) for a synthetic signal

$$\theta(t_k,\omega) \approx H(\ln(|\hat{W}(\omega)B(t_k,\omega)| + \mu A_{\max})), \tag{9}$$

in which $H(\ )$ denotes the Hilbert transform, A_{max} is the maximum of $|\hat{W}(\omega)B(t_k, \omega)|$, and μ is a small positive constant to avoid taking the natural logarithm of a zero value. Consequently, $\hat{R}_g(t_k, \omega)$ is given by

$$\hat{R}_g(t_k,\omega) = \frac{\hat{S}_g(t_k,\omega)}{|\hat{W}(\omega)B(t_k,\omega)| + \mu A_{\max}} e^{-i\theta(t_k,\omega)}. \tag{10}$$

Thus, the reflectivity series $r(t)$ is obtained by summing the inverse Gabor transform of $\hat{R}_g(t_k, \omega)$ over the POU windows

$$r(t) = \sum_{k=1}^{n} G^{-1}[\hat{R}_g(t_k,\omega)], \tag{11}$$

where n is the number of POU windows and G^{-1} is the inverse Gabor transform.

3. Models and Results

In this section, the preliminary results obtained from applying the Gabor algorithm to analytic data are presented and assessed. The metrics used to quantitatively assess the performance of the Gabor algorithm include 1) relative amplitude of recovered reflectivity; 2) polarity of recovered reflectivity; 3) location error in recovered reflectivity; and 4) extent of the response described as the full width at half of the maximal magnitude (FWHM). Gabor estimates of wavelets and reflectivity are determined to within an overall scale factor. Therefore, the relative strength of recovered reflectivity is a better indicator of the performance of Gabor algorithm than the absolute reflectivity. For the results shown in this section, the relative reflectivity is calculated as the ratio between the absolute reflectivity to the first recovered reflection coefficient. For example, assume the reflectivity series has three reflection coefficients, denoted as (r_1, r_2, r_3); then, the relative reflectivity is calculated as $(1, r_2/r_1, r_3/r_1)$. The polarity is the sign of recovered reflectivity, positive (+) or negative (-). The location error is the difference between the actual location and Gabor estimation. The FWHM is used to assess the signal resolution. At any location with a recognized reflection coefficient, FWHM is defined as the distance from the maximal magnitude to where the magnitude drops by half.

The model is designed to simulate uniform plane wave propagation in lossy and dispersive tissues over microwave frequencies. Our intention is to examine the ability of Gabor non-stationary deconvolution to compensate for attenuation loss and correct the phase dispersion. With this model, we can concentrate on the effects of attenuation and dispersion due to the dielectric properties, but eliminate the effects from other undesired factors (e.g., the attenuation due to geometric spreading in cylindrical or spherical wave propagation). As well, with a uniform plane wave, it is easy for us to have the exact solution of wave equation with which to compare the results.

The uniform plane wave solution of the wave equation for an electric field at a single frequency ω in one-dimension can be written as

$$E(x,t) = E_0 e^{-\alpha x} e^{i(\omega t - \beta x)}, \tag{12}$$

where α and β are the attenuation constant and the phase constant respectively. Given the biological tissues used in our experiments, these parameters are calculated using the properties obtained from the Cole-Cole model [11]. Table 1 lists the steps for signal generation and processing. Using the example of the uniform plane wave propagation in infiltrated fat [11], two sets of synthetic data were generated, one with an arbitrarily chosen sparse reflectivity series and the other with a randomly generated dense reflectivity series. Figure 2 illustrates the results with the dense reflectivity series. From top to bottom, the time series illustrates the true reflectivity, the recovered reflectivity using Gabor non-stationary deconvolution, the recovered reflectivity using Wiener stationary deconvolution, and the attenuated signal, respectively. It can be seen that a better match is observed between Gabor estimates and the true reflectivity in terms of relative reflectivity, polarity, location, and FWHM. Using the sparse reflectivity as an example, Table 2 compares the Gabor estimation and the estimation from Wiener stationary deconvolution.

Table 1 Work flow of data generation and processing

1. Given a location x, using equation (12), model the attenuation and dispersion in frequency domain.
2. Inverse Fourier Transform the output from step 1 to obtain the impulse response of attenuation and dispersion in time domain.
3. Convolve the impulse response with given source wavelet, which has minimum phase. The result describes the waveform of the propagating wavelet at location x in given lossy and dispersive medium.
4. For all required locations, repeat the above steps to construct a matrix that describes the waveform of the propagating wavelet at individual locations.
5. Generate a pseudo reflectivity series by either using a random data generator or arbitrarily choosing location and amplitude for reflectivity.
6. Multiply the matrix constructed in step 4 with the pseudo reflectivity series to get an attenuated signal.
7. Run Gabor nonstationary deconvolution with the attenuated signal.

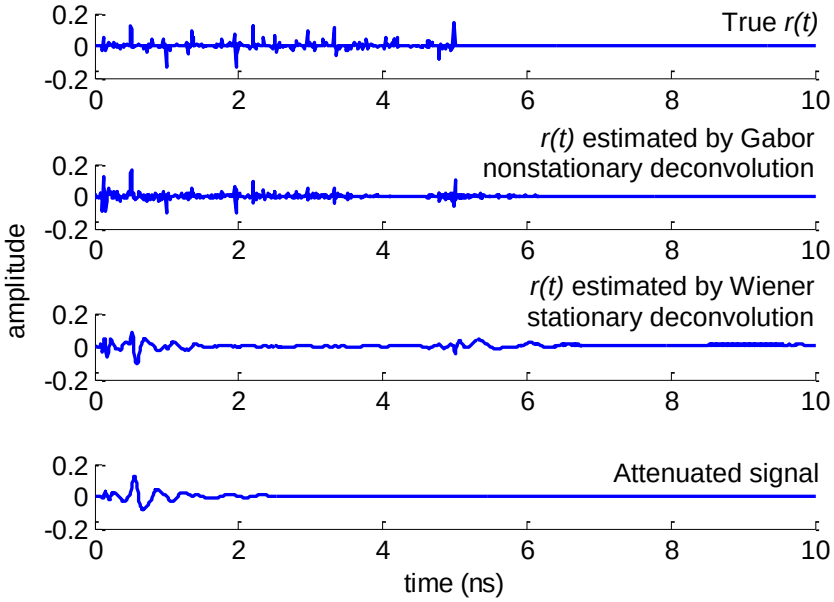

Figure 2 Gabor deconvolution with infiltrated fat over microwave frequency

Table 2 Differences between the Gabor estimation and the Wiener estimation

Metrics	Gabor Estimation	Wiener Estimation	Actual Reflectivity
Relative reflectivity	1, -1.53, 0.47, 0.18	1, -0.58, 0.075, -1.17	1, -1.5, 0.5, 0.25
Location error (mm)	0, 0, 0, 2	0, 0, 1, 0	0, 0, 0, 0
FWHM (mm)	2, 1, 1, 1.5	2.5, 0.02.5, 3, 2	N/A
Polarity of reflectivity	+, -, +, +	+, -, +, -	+, -, +, +

4. Conclusion

In this paper, we explored Gabor non-stationary deconvolution to recover the reflectivity function of imaged object in the presence of wavelet distortion due to the lossy and dispersive nature of breast tissues over microwave frequencies. We showed that the Gabor algorithm yields a very high-resolution estimate of the reflectivity on synthetic signals. Future work includes enhancement of the current Gabor process to make it more robust for processing radar signals and application of this algorithm to the measured data.

5. Acknowledgments

This work is financially supported by the Natural Sciences and Engineering Research Council (NSERC) of Canada and the University of Calgary. The authors also wish to thank the Consortium for Research in Elastic Wave Exploration Seismology (CREWES) for providing the software support.

6. References

[1] E. C. Fear, "Microwave imaging of the breast," *Technol Cancer Res Treat*, vol. 4, no. 1, pp. 69-82, Feb, 2005.

[2] O. Yilmaz, *Seismic Data Analysis: Processing, Inversion, and Interpretation of Seismic Data*, 2nd ed., Tulsa, OK, USA: Society of Exploration Geophysicists, 2001.

[3] S. Cloude, *An introduction to electromagnetic wave propagation and antennas*, UK: UCL Press, 1995.

[4] G. F. Margrave, M. P. Lamoureux, and D. C. Henley, "Gabor deconvolution: Estimating reflectivity by nonstationary deconvolution of seismic data," *Geophysics*, vol. 76, no. 3, pp. W15-W30, May-Jun, 2011.

[5] E. Kjartansson, "CONSTANT Q-WAVE PROPAGATION AND ATTENUATION," *Journal of Geophysical Research*, vol. 84, no. NB9, pp. 4737-4748, 1979.

[6] E. A. Robinsion, "Predictive decomposition of time series with applications to seismic exploration," Department of Geology and Geophysics, Massachusetts Institute of Technology (MIT), Cambridge, MA, US, 1954.

[7] W. I. Futterman, "DISPERSIVE BODY WAVES," *Journal of Geophysical Research*, vol. 67, no. 13, pp. 5279-&, 1962.

[8] J. F. Claerbout, *Fundamentals of geophysical data processing*: McGraw-Hill Inc.,US, 1976.

[9] V. V. Solodovnikov, *Introduction to the statistical dynamics of automatic control systems.*, New York: Dover Publications Inc., 1960.

[10] A. R. V. Hippel, *Dielectrics and Waves*, 2nd ed., New York, US: John Wiley & Sons, Inc, 1959.

[11] S. Gabriel, R. W. Lau, and C. Gabriel, "The dielectric properties of biological tissues .3. Parametric models for the dielectric spectrum of tissues," *Physics in Medicine and Biology*, vol. 41, no. 11, pp. 2271-2293, Nov, 1996.